Photoinduced Electron Transfer between C_{60} and *Bis*-Diphenylamino (Diphenylpolyenes), Measurement of Intrinsic Quantum Efficiency

Yanong Han and Lee H. Spangler*

Department of Chemistry, Montana State University, Bozeman, Montana 59717

Received: July 23, 2001

Intermolecular photoinduced electron transfer between C_{60} and two *bis*-diphenylamino (diphenylpolyenes) in dilute solutions was measured using step-scan Fourier transform spectroscopy which yielded extremely smooth temporal data. A mechanistic model containing a single intermediate and treatment of the kinetics generates a total quantum efficiency for free ions that can be factored into two terms, a quenching efficiency, Φ_Q, and an efficiency for formation of free ions out of the intermediate, Φ_{SI}. Two methods for extracting Φ_{SI} are provided and the dependence on solvent polarity and other parameters is investigated.

1. Introduction

Electron transfer (ET) between two species is a field of fundamental importance in biological photosynthesis and in materials work as well as a discipline with intrinsic scientific interest.[1−3] Photoinduced electron transfer (PET), studied by laser flash photolysis and time-resolved techniques, has led to a better understanding of general features of ET mechanisms, but several problems that have been identified still remain.[4] Frequently, there are difficulties in separating diffusional and electron-transfer contributions to the rate, and in some cases the nature of the charged state that is formed (whether it is a partial charge-transfer complex, an associated ion pair, or solvated ions) is not clear. A significant body of work has emerged that investigates organic donors in dilute solutions using C_{60} as a photoinduced acceptor.[5−24] C_{60} is convenient for this purpose for three reasons: it can be pumped at the doubled Nd:YAG wavelength of 532 nm; it undergoes efficient intersystem crossing to $^3C_{60}$* which is sufficiently long-lived to permit diffusion and donor−acceptor encounters to occur in dilute solution, and the $^3C_{60}$* is a reasonably strong acceptor.

The PET process is generally believed to follow a mechanism as shown in Scheme 1. The excited species diffuses, forms an encounter complex with the donor, then undergoes electron transfer eventually resulting in solvated ions. In dilute solution studies involving fullerenes, the lifetime of the $^3C_{60}$* typically shows a linear dependence on the donor concentration indicating that quenching of the excited triplet is a diffusion-limited process. Because the donor cation rise is dependent on the $^3C_{60}$* decay, it is often assumed that the overall electron-transfer process in dilute solution is diffusion-limited as well. However, it is known that electron-transfer rates vary over many orders of magnitude[25] so careful consideration of the influence of intermediates on the overall rate, and the quantum efficiency, may be warranted.

In this work, we investigate the kinetic treatment of diffusion-limited PET in dilute solutions and illustrate data treatment methods that separate forward and back ET[26] (BET) processes, and give a clearer indication of whether the overall mechanism is truly diffusion limited. This treatment also permits separation

SCHEME 1

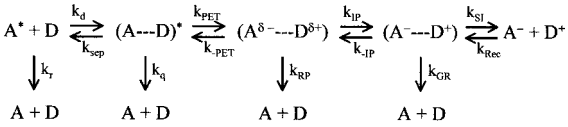

of the quantum efficiency of quenching from the quantum yield for formation of solvated ions from the intermediate, the latter perhaps being a truer measure of electron-transfer efficacy than the total quantum yield. Additionally, we report on use of step-scan Fourier transform photoinduced absorption methods[27−29] as a powerful experimental tool for study of PET and on two specific oligimers of a new class of organic electron donors, the *bis*-diphenylamino(diphenylpolyenes).[30]

2. Experimental Section

The bis-(diphenylamino)diphenylpolyenes used as electron donors in this study were synthesized by the Charles W. Spangler research group. C_{60} (acceptor) was obtained in a purity of 99.5% from Aldrich and used without further purification. Linear, ground-state absorption spectra were taken of solutions of C_{60} alone, donors alone, and both in solution together. Comparison of these spectra indicated no evidence of ground-state coupling.

All photoinduced absorption (PIA) measurements were performed in solution in 1 cm quartz cuvettes. Solutions were de-oxygenated by bubbling N_2 gas for 15 min resulting in $^3C_{60}$ lifetimes of around 22 μs (in C_{60} only solutions, without donor present). A 50 w continuous tungsten filament lamp was used as the broadband probe source and was focused with F/5 optics through the center of the cuvette. A Coherent Infinity Nd:YAG laser frequency doubled to 532 nm was used as a pump (typically 2 mJ/pulse) in a quasi-coaxial geometry with the probe light. After passing through the sample, the broadband light was refocused on an aperture where only the middle 20% of the laser spatial profile was sampled to reduce excitation gradients and their resulting problems, such as thermal lensing.

The light was then directed into a Bruker IFS 66 or IFS 88 step-scan interferometer to acquire the time and frequency resolved PIA spectrum. A Si diode or InSb (liquid N_2 cooled) detector and broad-band beam splitter were used in the experi-

* To whom correspondence should be addressed. Phone: (406) 994-4399. E-mail: lspangler@chemistry.montana.edu.

10.1021/jp012815f CCC: $20.00
Published on Web 11/16/2001

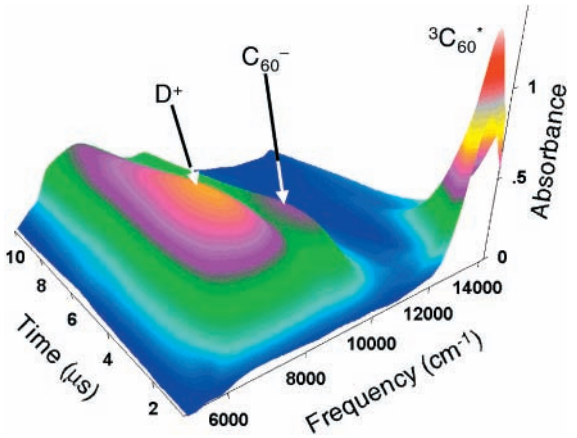

Figure 1. Time and frequency resolved photoinduced absorption (PIA) spectrum from the step-scan FT system for a solution of 0.25 mM C_{60} and 0.25 mM bis-(diphenylamino)diphenylethene ($n = 1$). The rapidly decaying peak centered at 13500 cm^{-1} is due to $^3C_{60}$* absorption. The broad, near-IR band which peaks at 6750 cm^{-1} is the intervalence band of the singly charged donor cation. The 9240 cm^{-1} band is the C_{60}^- absorption. The solvent used in this figure is a 1:1 *o*-dichlorobenzene/benzonitrile solvent mixture, but most of the following figures are in *o*-dichlorobenzene.

ments and the transient signals were acquired with a 12 bit, 40 MHz digitizer. The typical three-dimensional spectrum produced consisted of 400 traces with 200 or 300 cm^{-1} spectral resolution, and 25 or 50 ns temporal resolution generated by averaging 80 pulses at each interferometer mirror position.

3. Results and Interpretation

Figure 1 shows a typical time and frequency resolved photoinduced absorption (PIA) spectrum from the step-scan FT system for a solution of C_{60} and bis-(diphenylamino)diphenylethene ($n = 1$) in *o*-dichlorobenzene (o-DCB). At early times, the strong photoinduced absorption peak centered at ~13 400 cm^{-1} that dominates the spectrum is due to $^3C_{60}$* absorption for which the extinction coefficient is known.[19,31−33] As this peak decays, a very broad transition grows in the near-IR (6750 cm^{-1}) which can be attributed to the intervalence band[34] of D^+, the singly charged donor cation. This band is in the same region as other bis(triarylamine) intervalence bands[35] and its high degree of asymmetry indicates class III behavior, i.e., the charge is delocalized in the cation.[36] D^+ also shows an absorption band near 16,000 cm^{-1} and both the visible and IR absorptions have been confirmed by doping the donor with a strong oxidizing agent ($SbCl_5$) to chemically generate the cation. Also present in the spectrum is a 9240 cm^{-1} (1082 nm) peak which is the well-known C_{60}^- absorption.[19,37,38] Because extinction coefficients are known for both $^3C_{60}$* and C_{60}^-, these two species can be used to determine concentrations. Presence of the distinctive intervalence band, which will only exist in the singly charged species in these donors, and the C_{60}^- peak are proof of intermolecular electron transfer in this system. Shown in Figure 2 are spectral traces of $^3C_{60}$* and D^+ at early and late times which were extracted from the 3-D data set.

$^3C_{60}$* Decay. The D^+ spectrum has a broad peak centered in the visible whose tail slightly overlaps the $^3C_{60}$* absorption band. This contribution can be removed by scaling the D^+ intensity in this region at late times, long after the $^3C_{60}$* decay, to the intervalence band intensity. Then the intervalence temporal behavior scaled by this factor, is subtracted from the $^3C_{60}$* decay curve to provide a more accurate fit. The time-profiles of $^3C_{60}$* measured at 745 nm (Figure 3) indicate that the decay rates of

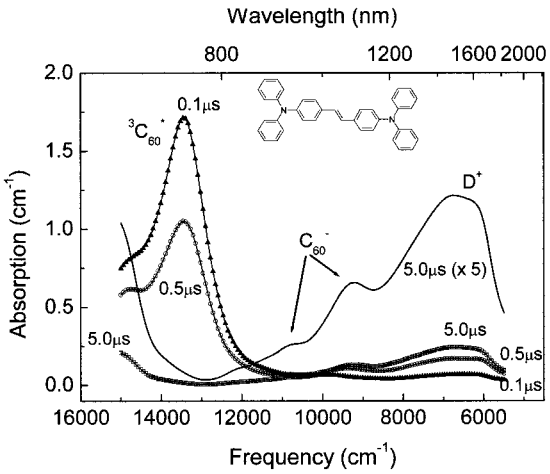

Figure 2. Spectral traces at different times extracted from a 3-dimensional time and frequency resolved data set similar to Figure 1. These data is for a solution of 0.2 mM C_{60} and 0.2 mM bis-(diphenylamino)-diphenylethene ($n = 1$) in *o*-dichlorobenzene solvent pumped by a 2 mJ, 5 ns 532 nm pulse.

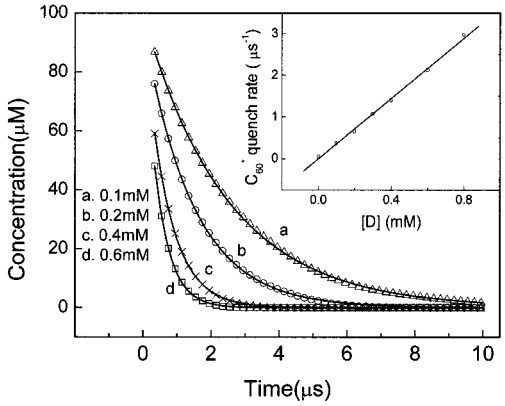

Figure 3. Main figure: $^3C_{60}$* decays as a function of donor ($n = 1$) concentration in ODCB; lines are exponential fits, points are experimental data. Only half the data points are plotted to allow the fit line to be seen. All solutions are in ODCB and pumped by a 2 mJ, 5 ns 532 nm pulse. Inset: Stern−Volmer plot of the decay rate vs donor concentration.

$^3C_{60}$* increase with increasing donor concentration. We can write the differential equation for the disappearance of the excited acceptor, A*

$$\frac{d[A^*]}{dt} = -k_r[A^*] - k_d[A^*][D] \qquad (1)$$

Measurement of the decay rate of $^3C_{60}$* in solution without the donor yields k_r. As mentioned above, the decay of $^3C_{60}$* in a solution containing donor, D, is also exponential, indicating that the second term in eq 1 is pseudo first order due to negligible changes in the donor concentration during the course of the reaction. Hence, eq 1 reduces to

$$\frac{d[A^*]}{dt} = -k_r[A^*] - k_Q[A^*] = -(k_r + k_Q)[A^*] \qquad (2)$$

where $k_Q = k_d[D]$. Integration yields the expected exponential decay

$$[A^*] = [A^*]_0 e^{-(k_r + k_Q)t} \qquad (3)$$

Measurement of the decay in the C_{60} with donor solution yields

SCHEME 2

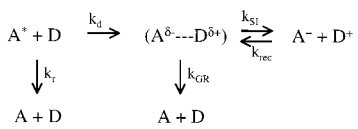

an observed rate constant that is

$$k_{obs} = k_r + k_Q = k_r + k_d[D] \quad (4)$$

where k_{obs} is the observed first-order decay rate constant of the triplet (fit with a single exponential), k_r is the rate constant without donor present, [D] is the concentration of the donor, and k_d is the bimolecular quenching rate constant A Stern−Volmer plot of k_{obs} vs [D] (inset of Figure 3) yields a straight line, which indicates that the *triplet quenching* is diffusion limited. A quenching rate constant of $k_d = 3.5 \times 10^9$ $M^{-1}s^{-1}$ was obtained from this fit.

Donor Cation Behavior. The data clearly suggest that the triplet quenching is diffusion limited, but that does not necessarily mean the entire electron-transfer process is. If we assume the *overall* reaction is diffusion limited, that means all processes for intermediates in Scheme 1 will be fast compared to k_d, and the time constant of the D^+ signal rise should be nearly equal to the $^3C_{60}$* decay ($\tau_{rise} \cong \tau_{decay}$ where $\tau_{decay} = 1/k_{decay}$). In such a case, it may not be possible to track the formation and concentrations of the intermediates even with high temporal resolution techniques because the relative rates will dictate very low concentrations of the intermediates at any time during the reaction. On the other hand, completely ignoring the existence of the intermediates will result in erroneous treatment of the source of certain efficiencies in the process. In this case, it becomes reasonable to approximate the mechanism with a simpler one that models multiple, undetectable intermediates in Scheme 1 with a single intermediate, as shown in Scheme 2. This has the advantage of simplifying the kinetic equations, retaining all measurable species, yet acknowledging that recombination processes for the intermediate ultimately affect quantum efficiency for formation of separated ions.

We now treat the kinetics for this simpler, approximate mechanism. The differential equations for the disappearance of A* still hold. A differential equation can also be written for the time dependence of the D^+ concentration

$$\frac{d[D^+]}{dt} = k_{SI}[I] - k_{rec}[A^-][D^+] \quad (5)$$

where [I] is the concentration of the intermediate, shown as ($A^{\delta-}$- - -$B^{\delta+}$) in the mechanism. If the steady-state approximation is applied to the intermediate, we have

$$\frac{d[I]}{dt} = 0 = k_d[A^*][D] + k_{rec}[A^-][D^+] - k_{SI}[I] - k_{GR}[I] \quad (6)$$

and

$$[I] = \left(\frac{k_d}{k_{SI} + k_{GR}}\right)[A^*][D] + \left(\frac{k_{rec}}{k_{SI} + k_{GR}}\right)[A^-][D^+] \quad (7)$$

Substitution into (4) yields

$$\frac{d[D^+]}{dt} = k_{SI}\left(\frac{k_d}{k_{SI} + k_{GR}}\right)[A^*][D] + k_{SI}\left(\frac{k_{rec}}{k_{SI} + k_{GR}}\right)[A^-][D^+] - k_{rec}[A^-][D^+] \quad (8)$$

The quantum efficiency for formation of solvated ions from the intermediate is

$$\Phi_{SI} = \frac{k_{SI}[I]}{k_{GR}[I] + k_{SI}[I]} = \frac{k_{SI}}{k_{GR} + k_{SI}} \quad (9)$$

Substitution into eq 8 generates

$$\frac{d[D^+]}{dt} = k_d\Phi_{SI}[A^*][D] + k_{rec}\Phi_{SI}[A^-][D^+] - k_{rec}[A^-][D^+] \quad (10)$$

or

$$\frac{d[D^+]}{dt} = k_d\Phi_{SI}[A^*][D] - k_{rec}[A^-][D^+](1 - \Phi_{SI}) \quad (11)$$

where k_d and k_{rec} are diffusion rate contants, and $k_{rec}(1 - \Phi_{SI}) = k_{bet}$ is the observed rate constant for back electron transfer. The quantity $k_d\Phi_{SI} = k_{et}$ is equivalent to the observed forward electron-transfer rate constant reported in some of the literature. It should be pointed out that the *specific* quantity $(1 - \Phi_{SI})$ in eq 11 arises because of the simplified mechanism, and this is one respect in which the second mechanism should be considered approximate that the relationship between k_{bet} and k_{rec} may have different factor than $1 - \Phi_{SI}$ if the dominant path to neutrals in the forward direction is different than in the reverse. However, this term is conceptually important in that it illustrates that the experimentally determined rate from a second-order plot does not yield the true k_{rec}, but instead yields a value modified by some forward term.

It is useful to look at the two terms in eq 11 in the light of what can be measured experimentally. At times long compared to the quenching lifetime, the concentration of the photoprepared species will be zero ($[A^*]_{t>5\times\tau decay} \approx 0$), eliminating the first term. Additionally, because of charge conservation, $[A^-] = [D^+]$. These two factors simplify the equation to

$$\frac{d[D^+]}{dt} = -k_{bet}[D^+]^2, (t > 5\tau_{decay}) \quad (12)$$

After integration this yields

$$\frac{1}{[D^+]_t} = k_{bet}t + \frac{1}{[D^+]_{tmax}} \quad (13)$$

Thus, at times long compared to the decay of $^3C_{60}$*, the BET and decay of the ion PIA signal should follow second-order kinetics. A plot of $1/[D^+]$ vs time yields a straight line with a slope of the observed BET rate constant of k_{bet} (Figure 4).

The rise in the ion signal is due to the first term in eq 11. As mentioned above, for a diffusion-limited process the time constant of the D^+ signal rise should be nearly equal to the $^3C_{60}$* decay ($\tau_{rise} \cong \tau_{decay}$). But a fit of the rise for the raw experimental data will not provide an accurate measure because of the recombination term in eq 11. Because we can measure the effect of the second term independently at long times, we

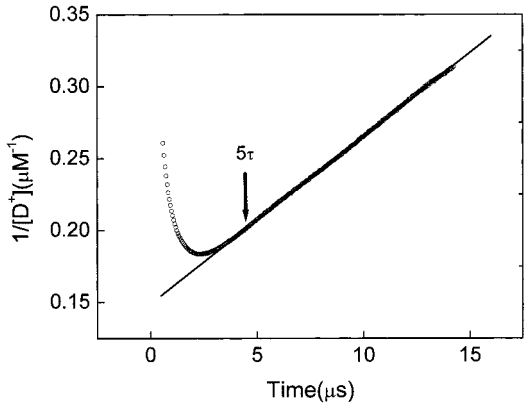

Figure 4. Plot of the inverse of the donor cation concentration vs time showing straight-line behavior after essentially complete decay of the excited acceptor ($^3C_{60}$*), marked as 5τ. The slope of this line is the observed back electron-transfer rate constant, k_{BET}. This second-order behavior indicates that the charged species detected in the experiment are solvated ions.

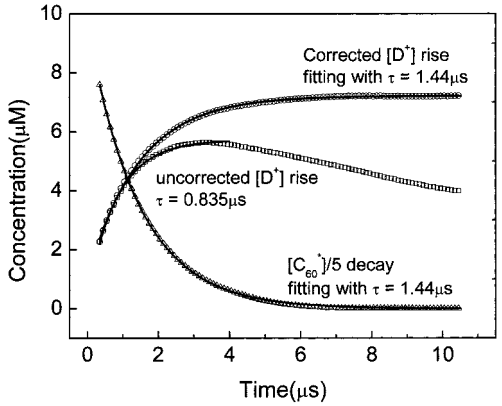

Figure 5. Decay of $^3C_{60}$* (÷5, triangles) compared to the rise of the bis-(diphenylamino)diphenylethene donor cation (D^+) along with fits (solid lines). Both the raw D^+ rise (squares) and the back electron transfer corrected rise (circles) are shown. Only half the data points are plotted to enable viewing of the fit lines. Eliminating the decay of the D^+ signal due to BET changes the best fit rise time constant significantly, and $\tau_{decay,\ C60} = \tau_{corrected\ rise,\ D+}$, indicating that the overall electron-transfer mechanism is diffusion limited.

can extrapolate this temporal behavior to early times and correct for the k_{bet} $[A^-][D^+]$ term resulting in the equation

$$\frac{d[D^+]}{dt} = k_d\Phi_{SI}[A^*][D] = k_Q\Phi_{SI}[A^*] \quad \text{(corrected to remove BET)} \quad (14)$$

Recalling that $[A^*]_t = [A^*]_0 e^{-(k_r + k_Q)t}$, eq 14 becomes

$$\frac{d[D^+]}{dt} = k_Q\Phi_{SI}[A^*]_0 e^{-(k_r + k_Q)t} \quad \text{(corrected for BET)} \quad (15)$$

Integration from $0 - t$ yields

$$[D^+]_t = \frac{k_Q}{k_r + k_Q}\Phi_{SI}[A^*]_0\{1 - e^{-(k_r + k_Q)t}\} \quad \text{(corrected for BET)} \quad (16)$$

given that $[D^+]_{t=0} = 0$.

Thus, we see that if we assume a diffusion-limited mechanism, the argument for the exponential rise of the cation is identical to that of the decay of the excited acceptor in eq 3 *if the data is corrected for BET*. This provides a good criterion for determination of whether the process is diffusion limited, but use of uncorrected data will not provide an accurate determination, as illustrated in Figure 5. We compared the rise of the D^+ signal and the decay of $^3C_{60}$*. For corrected data these values are in good agreement within 4%, but without the BET correction, the errors are approximately 40%, (Table 1).

We now define some additional useful quantum efficiencies. The quantum efficiency for production of the intermediate from the photoexcited species is the same as the quantum efficiency for quenching for the simplified mechanism

$$\Phi_Q = \frac{k_Q}{k_Q + k_r} \quad (17)$$

The overall quantum efficiency for production of solvated ions from $^3C_{60}$* is the product of Φ_{SI} and Φ_Q

$$\Phi = \Phi_{SI}\Phi_Q = \frac{k_{SI}}{k_{GR} + k_{SI}} * \frac{k_Q}{k_Q + k_r} \quad (18)$$

This factoring of total quantum yield into two components is similar to the treatment by von Raumer *et al.*[39] and substitution into eq 16 yields

$$[D^+]_t = \Phi[A^*]_0\{1 - e^{-(k_r + k_Q)t}\} \quad \text{(corrected for BET)} \quad (19)$$

Equation 18 also suggests a method of determining the total quantum efficiency. If we take time, $t \rightarrow \infty$, D^+ will have its maximum value and the exponential term will equal zero. We then see

$$[D^+]_{tmax} = \Phi\ [A^*]_0 \text{ or } \Phi = \frac{[D^+]_{tmax}}{[A^*]_{max}} \quad \text{(corrected for BET)} \quad (20)$$

TABLE 1: Rate Constants, Lifetimes and Quantum Efficiencies for Photoinduced Electron Transfer between C_{60} at 0.25 MM and *Bis*-Diphenylamino(diphenylstilbene) (n = 1), and *Bis*-Diphenylamino(diphenylbutadiene), (n = 2) at Several Different Concentrations[a]

[n = 1]	0.1 (mM)	0.2 (mM)	0.3 (mM)	0.4 (mM)
k_{bet} ($M^{-1}s^{-1}$)	1.2×10^{10}	1.3×10^{10}	1.4×10^{10}	1.3×10^{10}
τ_{decay} (s)	2.5×10^{-6}	1.4×10^{-6}	0.90×10^{-6}	0.69×10^{-6}
$\tau_{rise-raw}$ (s)	1.4×10^{-6}	0.87×10^{-6}	0.61×10^{-6}	0.42×10^{-6}
$\tau_{rise-corr}$ (s)	2.4×10^{-6}	1.4×10^{-6}	0.89×10^{-6}	0.67×10^{-6}
Φ_Q (%)	88.8	93.5	95.9	96.9
Φ_{SI} (%)	7.6	7.7	7.4	7.2
Φ_Q*Φ_{SI} (%)	6.8	7.2	7.2	7.0
Φ_{uncorr} (%)	5.0	5.8	6.1	6.1
Φ_{corr} (%)	6.8	7.3	7.4	7.0
[n = 2]	0.1mM	0.2mM	0.3mM	0.4mM
k_{bet} ($M^{-1}s^{-1}$)	8.6×10^9	8.6×10^9	8.7×10^9	8.6×10^9
τ_{decay} (s)	2.0×10^{-6}	1.0×10^{-6}	0.74×10^{-6}	0.57×10^{-6}
$\tau_{rise-raw}$ (s)	1.2×10^{-6}	0.67×10^{-6}	0.48×10^{-6}	0.36×10^{-6}
$\tau_{rise-corr}$ (s)	2.0×10^{-6}	1.0×10^{-6}	0.72×10^{-6}	0.573×10^{-6}
Φ_Q (%)	90.3	95.3	96.6	97.4
Φ_{SI} (%)	11.2	11.1	11.2	11.0
Φ_Q*Φ_{SI} (%)	10.2	10.5	10.9	10.7
Φ_{uncorr} (%)	7.5	8.6	9.1	9.4
Φ_{corr} (%)	10.1	10.6	10.9	10.8

[a] There are three quantities reported for total quantum efficiency: Φ_{uncorr}, which is obtained from the uncorrected maximum value method and is expected to give a value that is too low; Φ_{corr}, obtained from the corrected maximum value and should be accurate; and (Φ_Q*Φ_{SI}), obtained from the quenching rate and the first derivative plot and which should yield the same value as Φ_{corr}.

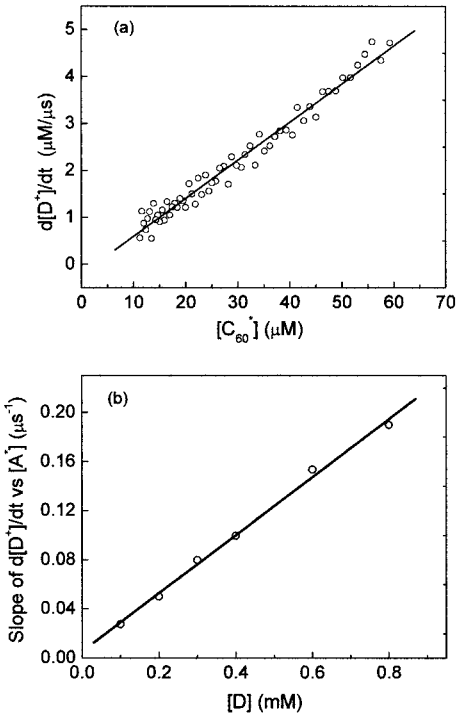

Figure 6. (a) Plot of d[D^+]/dt vs [$^3C_{60}$*] using BET corrected D^+ data for a 0.2 mM solution in both donor and C_{60} in ODCB. Equation 14 indicates that this plot has a slope of $k_d\,\Phi_{SI}$ [D] or $k_Q\Phi_{SI}$. (b) A plot of slopes determined by the method in part (a) vs donor concentration, analogous to a Stern−Volmer plot. The plot shows excellent linearity. The [D] dependence is due to the k_Q term in the slope and Φ_{SI} is independent of [D].

Note that $[A^*]_0$ is a maximum value and that $[D^+]_{t\ max}$ is the theoretical maximum ion concentration obtained by correcting for back electron transfer, not the maximum value in the raw experimental data. Figure 5 illustrates that the experimental and theoretical maxima can differ significantly.

We see that the total quantum efficiency contains Φ_Q, which will be strongly dependent on the diffusion rate and the lifetime of the photoprepared species. These properties are not relative to the intrinsic ET properties of the donor−acceptor system. It is desirable to determine the quantum efficiency of electron transfer from the intermediate, $\Phi_{SI} = k_{SI}/(k_{SI} + k_{GR})$. In dilute solution diffusion limited cases, the intermediate typically will not be measurable so the rate constants k_{SI} and k_{GR} may not be directly determined. But Φ_{SI} can be determined via two methods. The first method, which we will refer to as the maximum value method, uses eq 19 to determine the total quantum efficiency, and lifetime measurements to calculate Φ_Q from k_Q and k_r. Φ_{SI} is then determined from eq 18.

The second method determines Φ_{SI} from a plot the first derivative of the BET corrected cation concentration vs [A*] as in eq 14. A plot of d[D^+]/d*t* vs [$^3C_{60}$*] will have a slope of $k_d\Phi_{SI}$ [D] or $k_Q\Phi_{SI}$. Because k_Q was determined from the $^3C_{60}$* decay and eq 4 this first derivative plot ultimately yields Φ_{SI}, the desired quantity (Figure 6 a). Because even moderate fluctuations will result in a first derivative plot with very large scatter and a poorly determined slope, this method of determining Φ_{SI} requires time-resolved data with very low noise. In a method analogous to a Stern−Volmer plot, the slopes determined by the first derivative method for several experiments run at different concentrations can be plotted vs [D] which will result in a slope of $k_d\,\Phi_{SI}$. (See Figure 6b.) An actual Stern−Volmer plot of the same data yields k_d, so the ratio between the two provides Φ_{SI}.

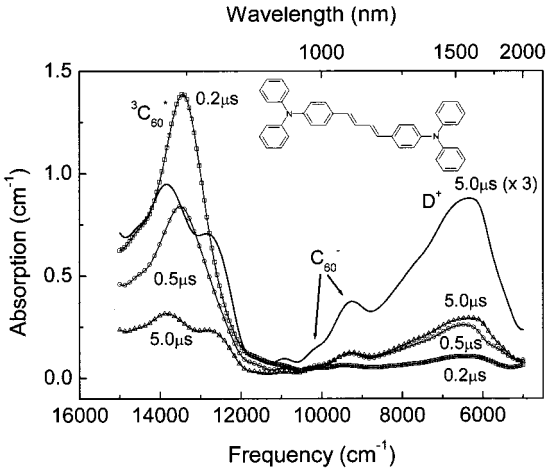

Figure 7. PIA spectra at various times extracted from a 3-D data set for a 0.2 mM C_{60}/ bis-(diphenylamino)diphenylbutadiene) ($n = 2$) solution in ODCB.

TABLE 2: Solvent Polarity Dependence Data, 0, 25%, 50% Benzonitrile (BN) in *o*-dichlorobenzene (ODCB)[a]

BN in ODCB	0	25%	50%
dielectric constant	9.93	13.87	17.82
k_{bet} ($M^{-1}s^{-1}$)	1.2×10^{10}	6.2×10^{9}	5.2×10^{9}
τ_{decay} (s)	1.1×10^{-6}	1.0×10^{-6}	1.0×10^{-6}
$\tau_{rise-corr}$ (s)	1.0×10^{-6}	0.9×10^{-6}	1.1×10^{-6}
Φ_Q (%)	95.2	95.3	95.6
Φ_{SI} (%)	7.7	18.6	26.5
$\Phi_Q{}^*\Phi_{SI}$ (%)	7.3	17.7	25.4
Φ_{uncorr} (%)	5.9	14.0	18.5
Φ_{corr} (%)	7.1	17.3	24.3

[a] Solutions are 0.25 mM in both C_{60} and *bis*-diphenylamino(diphenylstilbene) ($n = 1$).

The same processes were performed with C_{60}/ bis-(diphenylamino)diphenylbutadiene) ($n = 2$). The transient PIA spectrum shows indicates that there is electron transfer from the $n = 2$ donor to $^3C_{60}$*. The $n = 2$ donor cation shows a similar intervalence band in the IR, but the visible absorption band is red shifted compared to the stilbene (see Figure 7). Table 1 shows rate constants and quantum efficiencies for two different donors (bis-(diphenylamino)diphenylethene and bis-(diphenylamino)diphenylbutadiene) at four different concentrations. In all cases, the $^3C_{60}$* decay and the D^+ rise exhibit the same time constant to within experimental error indicating the electron-transfer process is, indeed, diffusion limited. The two methods of determining Φ_{SI} yield results that are in good agreement with each other.

In order to further test the kinetic treatment and the outlined method of analysis, conditions were changed to produce changes in the two quantum efficiency terms, Φ_Q and Φ_{SI}. In the first case, data were collected as a function of solvent polarity using mixtures that were 0%, 25%, and 50% benzonitrile (BN) in *o*-DCB with 0.25mM concentration of both C_{60} and bis-(diphenylamino)diphenylethene. Higher polarity solvents stabilize the intermediate and the solvated ions so will typically increase Φ_{SI}. This solvent change will have a relatively small effect on the diffusion rate of the neutral species or the lifetime of $^3C_{60}$*, so Φ_Q should not be strongly effected. Rates and quantum efficiencies for the electron-transfer process were determined and extracted by the methods outlined above (Table 2), and a significant change in Φ_{SI} is observed ranging from 7.4% in ODCB to 26.5% in a 1:1 mixture of ODCB/BN. The quenching efficiency remains at ~0.95 for all three solutions.

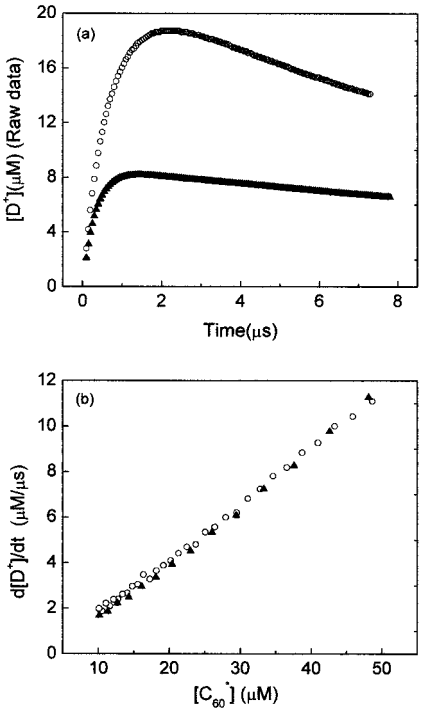

Figure 8. (a) Uncorrected D^+ behavior for a 0.25 mM bis-(diphenylamino)diphenylethene, C_{60} solution in a 1:1 ODCB/BN solvent pumped with 0.2 mJ pulses with (open circles) and without (black triangles) deoxygenation. Quenching by oxygen strongly affects total ion yield. (b) First derivative plots (as in Figure 6) for BET corrected part (a) data. Because both the psuedo-first order *donor* quenching rate constant, k_Q, and the quantum efficiency for formation of solvated ions from the intermediate, Φ_{SI}, are unaffected by the oxygen, the slopes of the two first derivative plots are essentially identical.

Additionally, Φ_{SI} values determined via the maximum value method and the first derivative plot method are in reasonable agreement.

Because the lifetime of $^3C_{60}$* is long compared to the diffusion process,[4,40] Φ_Q is typically close to 1 when C_{60} is used as the photoinduced acceptor. The total quantum yield will then have a value close to Φ_{SI}, as is observed in the data presented in Tables 1 and 2. For photoinduced species with shorter lifetimes, or for systems with much slower diffusion rates, separation of the contributions of Φ_Q and Φ_{SI} can yield information about the efficacy of charge state formation. To illustrate this point, we changed the degree to which we deoxygenated solutions and performed new measurements. By changing the degree of deoxygenation, k_r is effectively increased, making it more competitive with k_Q and reducing the value of Φ_Q. Because the intermediates in the electron transfer mechanism are relatively short lived, they should be relatively insensitive to dissolved oxygen concentration and we would anticipate that Φ_{SI} would not change appreciably. We measured the transient absorption of a solution of [bis-(diphenylamino)-diphenylethene] = [C_{60}] = 0.25 mM in a 1:1 ratio of ODCB/BN solvent at same laser pump power with, and without deoxygenation of the solution. Figure 8 shows a plot of the first derivative of the BET corrected cation concentration vs [A*] under these two conditions. Neither the slope, $k_Q\Phi_{SI}$, nor the initial [$^3C_{60}$*] changes. Kinetic data is given in Table 3 which shows that the total quantum efficiency drops from ~0.25 to ~0.09 without deoxygenation, but Φ_{SI} is unchanged to within 2% as measured by the first derivative method. The change in total quantum efficiency is due to a reduction of Φ_Q from 0.95 to 0.32.

TABLE 3: Deoxygenation Dependence Data. Solutions Are 0.25 MM in Both C_{60} and $n = 1$ in a 50/50 ODCB/BN Solvent

status	deoxygenated (bubbled N_2 gas)	not deoxygenated (no bubbling)
k_{bet} ($M^{-1}s^{-1}$)	5.2×10^9	5.4×10^9
τ_{decay} (s)	0.98×10^{-6}	0.43×10^{-6}
$\tau_{rise-corr}$ (s)	1.1×10^{-6}	0.40×10^{-6}
Φ_Q (%)	95.6	32.5
Φ_{SI} (%)	26.5	27.3
$\Phi_Q*\Phi_{SI}$ (%)	25.3	8.9
Φ_{uncorr} (%)	18.5	8.1
Φ_{corr} (%)	24.3	8.8

4. Discussion

It is tempting to assume that PET in dilute solutions will be diffusion limited because the encounter between the photoprepared species and the partner species will be. However, ET rates in other systems can vary over many orders of magnitude and can occur over fairly long distances,[1,3,25] so a test of this assumption is warranted. When a diffusion-limited mechanism is assumed, and treated kinetically, several issues arise that will be discussed in detail in this section.

Test Criterion for Diffusion-Limited Behavior. In the previous section, it was shown that the time constant for the rise of the ion signal should equal that of the photoinitiator decay. This is not at all surprising, but what is easy to overlook is that the ion signal decay due to BET must somehow be taken into account to get a reliable determination. In this work, it is accomplished by fitting the BET at long times, extrapolating to early times and subtracting. Another approach is to numerically model the ion signal dependence and extract τ_{rise}. This correction is critical for other factors discussed below.

If the process is not diffusion limited, τ_{rise} for the cation will be less than τ_{decay} for the photoinitiator, and a measurable population might exist in one or more of the intermediate states shown in the first mechanism (Scheme 1). This intermediate signal should peak before the solvated ion signal, but may be very difficult to extract because it may highly overlap either the photoinitiator signal, or the solvated ion signal, depending on which intermediate has the longest lifetime.

Measurement of Quantum Efficiency. The ratio of the maximum [D^+] value in the raw experimental data to $[A^*]_{max}$ is sometimes used as a measure of quantum yield. This method generates a quantum yield at one specific time; the point at which forward and back ET are balanced. (Ultimately, the quantum yield is zero because the ions recombine.) We have shown that by correcting for BET and using the corrected maximum value of [D^+], a quantum *efficiency* related-to-branching ratios of rate constants (eqs 19 and 17) can be determined that provides the fraction of photoexcited species that go on to transfer an electron.

In the simplified, diffusion-limited mechanism, there are two contributions to this yield, the fraction of photoexcited species that undergo an encounter with the donor before relaxation, Φ_Q, and the fraction of intermediates that go on to form solvated ions, Φ_{SI}. The Φ_Q term is dictated by the lifetime of the photoexcited species and the diffusion rate whereas the second term is a better measure of the *intrinsic* ET behavior. The data presented above for solutions that were not deoxygenated in order to effectively increase k_r and reduce Φ_Q, illustrate this point clearly. The result of this experiment is that the reduction in Φ_Q results in fewer A* − D encounters and a reduction of overall quantum efficiency. But Φ_{SI} remains the same within experimental error, indicating that for the A* − D encounters

that do occur, the same fraction go on to form solvated ions. The kinetic treatment presented here shows that even if the intermediate cannot be measured, Φ_{SI} can be extracted from PET data by two different methods.

Back Electron Transfer. Equation 12 shows that recombination of the solvated ions should follow second-order kinetics as expected, but a plot of $1/[D^+]$ vs t yields a slope of $(1 - \Phi_{SI})\ k_{rec}$, not a true rate constant. The specific $(1 - \Phi_{SI})$ term occurs because recombination (BET) causes re-formation of the intermediate. In the simplified second mechanism, the intermediate can then either undergo geminate recombination, or it can go forward again to form solvated ions with a branching ratio of Φ_{SI}. In a mechanism with only one intermediate, this term will look identical to the forward term, but in a more realistic mechanism, such as in Scheme 1, the dominant path to neutrals in the forward direction might be different than in the reverse direction. This would occur if k_{RP} and k_{GR} are both greater than k_{IP} and k_{-IP}, resulting in a quantity other than $(1 - \Phi_{SI})$ modifying the recombination rate constant. This can be true even in a diffusion limited ET process. If all other rates in the first mechanism are significantly faster than k_{diff} and k_{rec}, the process will be diffusion limited. But if the relationship between k_{RP}, k_{GR}, k_{IP}, and k_{-IP} mentioned holds, the dominant path to neutrals will be different in the forward and reverse directions so the $(1 - \Phi_{SI})$ would be incorrect. This is the main consequence of approximating multiple intermediates with one in a diffusion-limited mechanism. However, even if the more complicated mechanism is correct, the slope of the second derivative plot still would *not* yield a true rate constant because it would contain some branching ratio term as a consequence of re-formation of solvated ions.

Whatever the appropriate branching ratio or quantum efficiency is in this term, it can potentially have a dramatic consequence on the effective recombination rate. If the branching ratio approaches one, recombination will slow significantly and the ion species will be very long-lived.

5. Summary and Conclusions

Photoinduced electron transfer of two *bis*-diphenylamino-(diphenylpolyenes) with C_{60} as the photoinduced acceptor was measured using step-scan FT transient absorption techniques. The method yielded data with exceptional signal-to-noise ratio that was simultaneously both temporally and spectrally resolved (as opposed to resolved in one dimension and sampled in the other). The quality and completeness of this type of data set allows for accurate spectral and temporal traces to be extracted even in cases where there is significant overlap of spectral transitions.

Also presented was a kinetic treatment of a diffusion-limited mechanism. The mechanism used acknowledges that the intermediates will play a role in the quantum efficiency of solvated ion formation, but is approximate in the sense that it only contains one intermediate. This explicit treatment of an intermediate is in contrast to the formalism used in much of the dilute solution PET literature, and it yields some useful new features. Key among these are as follows: identification of a criterion for determination of whether the entire ET process (as opposed to just the photoinitiator quenching) is diffusion limited; a better measure of the total quantum efficiency that is related to the relevant rate constants; a quantum efficiency for formation of ions out of the intermediate that is a truer measure of the intrinsic ET efficacy of the system than is the total quantum yield; and the importance of properly correcting for BET in order to determine many of these quantities. The data reduction methods required to generate this information were also presented.

Acknowledgment. The authors would like to thank Mr. Ben Reeves and Dr. Charles Spangler for provision of the donors used in this investigation. This material is based upon work supported in part by the U. S. Army Research Laboratory and the U. S. Army Research Office under Grant No. DAAD19-00-1-0162. We also thank Scientific Materials Corp. for partial support of this work.

References and Notes

(1) Chanon, M.; Fox, M. A. *Photoinduced Electron Transfer*; Elsevier: New York, 1988.

(2) Fox, M. A. *Chem. Rev.* **1992**, *92*, 365.

(3) Jortner, J.; Bixon, M. Advances in Chemical Physics, Vol. 106, *Electron Transfer—From Isolated Molecules to Biomolecules*, Pt. 1, Vol. 106; John Wiley & Sons: New York, 1999; Jortner, J.; Bixon, M. Advances in Chemical Physics, Vol. 106, Electron Transfer- -From Isolated Molecules to Biomolecules, Pt. 2, Vol. 107; John Wiley & Sons: New York, 1999.

(4) Zanini, G. P.; Montejano, H. A.; Cosa, J. J.; Previtali, C. M. *J. Photochem. Photobio. A: Chem.* **1997**, *109*, 9.

(5) Arbogast, J. W.; Darmanyan, A. P.; Foote, C. S.; Rubin, Y.; Diederich, F. N.; Alvarez, M. M.; Anz, S. J.; Whetten, R. L. *J. Phys. Chem.* **1991**, *95*, 11.

(6) Arbogast, J. W.; Foote, C. S.; Kao, M. *J. Am. Chem. Soc.* **1992**, *114*, 2277.

(7) Nonell, S.; Arbogast, J. W.; Foote, C. S. *J. Phys. Chem.* **1992**, *96*, 4169.

(8) Palit, D. K.; Ghosh, H. N.; Pal, H.; Sapre, A. V.; Mittal, J. P.; Seshadri, R.; Rao, C. N. R. *Chem. Phys. Lett.* **1992**, *198*, 113.

(9) Ghosh, H. N.; Pal, H.; Sapre, A. V. *J. Am. Chem. Soc.* **1993**, *115*, 11 722.

(10) Guldi, D. M.; Hungerbuhler, H.; Janata, E.; Asmus, K.-D. *J. Chem. Soc., Chem. Commun.* **1993**, 84.

(11) Guldi, D. M.; Hungerbuhler, H.; Janata, E.; Asmus, K.-D. *J. Phys. Chem. A*, **1993**, *97*, 11 258.

(12) Guldi, D. M.; Hungerbuhler, H.; Asmus, K. D. *J. Phys. Chem.* **1995**, *99*, 9380.

(13) Guldi, D. M.; Hungerbuhler, H.; Asmus, K. D. *J. Phys. Chem.* **1995**, *99*, 13 487.

(14) Guldi, D. M.; Asmus, K. D. *J. Phys. Chem. A* **1997**, *101*, 1472.

(15) Guldi, D. M.; Hungerbuhler, H.; Asmus, K. D. *J. Phys. Chem. A* **1997**, *101*, 1783.

(16) Mikami, K.; Matsumoto, S.; Ishida, A. *J. Am. Chem. Soc.* **1995**, *117*, 11 134.

(17) Biczok, L.; Linschitz, H. *J. Phys. Chem.* **1995**, *99*, 1843.

(18) Biczok, L.; Gupta, N.; Linschitz, H. *J. Am. Chem. Soc.* **1997**, *119*, 12 601.

(19) Biczok, L.; Linschitz, H.; Walter, R. I. *Chem. Phys. Lett.* **1992**, *195*, 399.

(20) Steren, C. A.; van Willigen, H.; Biczok, L.; N. Gupta, N.; Linschitz, H. H. *J. Phys. Chem.* **1996**, *100*, 8920.

(21) El-Kemary, M.; Fujitsuka, M.; Ito, O. *J. Phys. Chem. A* **1999**, *103*, 1329.

(22) El-Kemary, M.; El-Khouly, M.; Fujitsuka, M.; Ito, O. *J. Phys. Chem. A* **2000**, *104*, 1196.

(23) Serpa, C.; Arnaut, L. G. *J. Phys. Chem. A* **2000**, *104*, 11 075.

(24) Weng, X. Y.; Chan, K. C.; Tzeng, B. C.; Che, C. M. *J. Chem. Phys.* **1998**, *109*, 5948.

(25) Kavarnos, G. J. *Fundamentals of Photoinduced Electron Transfer*; John Wiley & Sons: New York, 1993.

(26) Weidemaier, K.; Tavernier, H. L.; Swallen, S. F. J.; Fayer, M. D. *J. Phys. Chem. A* **1997**, *101*, 1887.

(27) Connes, J.; Connes, P. J. *J. Opt. Soc. Am.* **1996**, *56*, 896.

(28) Manning, C. J.; Palmer, R. A.; Chao, J. L. *Rev. Sci. Inst.* **1991**, *62*, 1219.

(29) Hartland, G. V.; Xie, W.; Dai, H. L.; Simon, A.; Anderson, M. J. *Rev. Sci. Inst.* **1992**, *63*, 3261.

(30) Reeves, B.; Spangler, C. S., in preparation.

(31) Kajii, Y.; Nakagawa, T.; Suzuki, S.; Achiba, Y.; Obi, K.; Shibuya, K. *Chem. Phys. Lett.* **1991**, *181*, 2.

(32) Sension, R. J.; Phillips, C. M.; Szarka, A. Z.; Romanow, W. J.; McGhie, A. R.; McCauley, J. P., Jr.; Smith, A. B.; Hochstrasser, R. M. *J. Phys. Chem.* **1991**, *95*, 6075.

(33) Dimitrijevic, N. M.; Kamat, P. V. *J. Phys. Chem.* **1992**, *96*, 4811.

(34) Hush, N. S. *Prog. Inorg. Chem.* **1967**, *8*, 391. (b) Hush, N. S. *Coord. Chem. Rev.* **1985**, *64*, 135.
(35) Lambert, C.; Noll, G. *J. Am. Chem. Soc.* **1999**, *121*, 8434.
(36) Robin, M.; Day, P. *Adv. Inorg. Radiochem.* **1967**, *10*, 247.
(37) Heath, G. A.; McGrady, J. E.; Martin, R. L. *J. Chem. Soc., Chem. Commun.* **1992**, 1272.
(38) Lawson, D. R.; Feldheim, D. L.; Foss, C. A.; Dorhout, P. K.; Elliott, C. M.; Martin, C. R.; Parkinson, B. *J. Electrochem. Soc.* **1992**, *139*, L68.
(39) Von Raumer, M.; Sarbach, A.; Haselbach, E.. *J. Photochem. Photobio. A: Chem.* **1999**, *121*, 75.
(40) Fraelich, M. R.; Weisman, R. B. *J. Phys. Chem.* **1993**, *97*, 11 145.